Molecular dynamics simulations of polymer droplets

Lukas Wagner
Department of Physics, Ohio State University, Columbus, Ohio 43210
(Received 29 September 1994)

We have simulated droplets of chain molecules of length 4 and 16 adsorbed on a van der Waals substrate using molecular dynamics. We investigate the behavior of individual chains in equilibrium droplets and in spreading droplets, and roughly characterize the macroscopic dynamics of spreading droplets.

PACS number(s): 61.20.Ja, 61.41.+e, 68.10.Gw, 68.45.Gd

A number of recent experimental studies have investigated the spreading of nonvolatile polymer droplets. Various phenomena associated with the existence of atomic monolayers in such droplets are among the most novel features of these studies [1–4]. Previous theoretical work on both static and dynamic properties of droplets has largely treated droplets as continuous objects ([5], and references therein). A notable exception is the theory of de Gennes and Cazabat [6], which treats the spreading of a droplet of simple liquid made of discrete atomic layers. This work presents various results from simulations of mesoscopic nonvolatile droplets, including evidence of layering and a test of the predictions of the theory of [6] for such droplets.

The atoms in our simulations exert two types of forces on each other: (1) the forces due to a truncated, shifted Lennard-Jones (LJ) potential,

$$V(r) = 4\epsilon\left[\left(\frac{\sigma}{r}\right)^{12} - \left(\frac{\sigma}{r_C}\right)^{12} - \left(\frac{\sigma}{r}\right)^{6} + \left(\frac{\sigma}{r_C}\right)^{6}\right]$$

for $r \le r_C$ and $V(r) = 0$ for $r > r_C = 2\sigma$, and (2) forces of constraint which maintain a fixed distance between neighbors on a chain of given length N_c. Modeling a carbon chain, appropriate length and time scales for our simulations are $\sigma \sim 4.1$ Å and $\tau = \sqrt{m\sigma^2/\epsilon} \sim 3 \times 10^{-12}$ s.

We implement the LJ forces in standard fashion, by using a linked-list-based program for three-dimentional (3D) short-ranged potential molecular dynamics [7,8]. We implement the constraint forces using the method of Ryckaert *et al.* [9] to impose rigid bonds of length 1.125σ between atoms. Briefly, the idea is to calculate the unconstrained motion of all the atoms, and then to find and impose forces of constraint just sufficient to keep the separation between neighbors in a chain constant, a method we found to be easy to implement and quite efficient as no fast vibrational time scale is introduced. We impose no bond-bending forces. We use the "Verlet method" to integrate the equations of motion, with a time step of $h = \tau/141$. As a gauge of the numerical accuracy of our simulations, in the microcanonical ensemble we find energy fluctuations with a standard deviation of 10^{-4} times the difference between kinetic and potential energies. For simulations in which a droplet spreads on a substrate, we impose constant mean kinetic energy by rescaling velocities. For equilibrium simulations, we find no differences between droplets simulated in the microcanonical ensemble and droplets simulated with velocity rescaling, which is not too surprising in light of a similar observation by Thompson *et al.* for droplets of simple liquid [10].

The surface with which these chains interact is a uniform, semi-infinite slab of LJ material. The potential which such a material produces, again truncated and shifted, is

$$V(z) = 4\pi\epsilon_w\left(\frac{\sigma_w}{\sigma}\right)^3\left\{\frac{1}{45}\left[\left(\frac{\sigma_w}{z}\right)^9 - \left(\frac{\sigma_w}{z_C}\right)^9\right] - \frac{1}{6}\left[\left(\frac{\sigma_w}{z}\right)^3 - \left(\frac{\sigma_w}{z_C}\right)^3\right]\right\}$$

for $z \le z_C$, and $V(z) = 0$ for $z > z_C = 2\sigma$. For all simulations discussed here, $\sigma_w^* \equiv \sigma_w/\sigma = 1.2$. Note that the force due to this potential is purely in the z direction so that there are no frictional effects arising from motion parallel to the surface.

We prepared the initial condition for our simulations as follows. One hundred chains with $N_c = 16$ were created in an arbitrary initial low-density configuration in a container with repulsive walls. The chains attracted each other, and coalesced to form a droplet. This coalescing took place with periodic velocity rescaling to keep the mean kinetic energy constant. Once the chains formed a single cluster, an equilibration period of 3500τ followed. The equilibrated polymer droplet was then brought into contact with a surface whose attractive potential is weak enough that the droplet does not wet it, and is again allowed to equilibrate for 3500τ. This equilibrated droplet on a surface is our initial state. Independent but macroscopically equivalent initial states may be obtained by storing the microstate at later times in the equilibrium simulation. To generate initial conditions for a different substrate or different temperature from this state, or for droplets made of shorter chains (as long as the new length divides the old one), requires only an equilibration period for the new configuration.

A typical equilibrated droplet configuration with $N_c = 16$, $T^* \equiv kT/\epsilon = 0.75$, and $\epsilon_w^* \equiv \epsilon_w/\epsilon = 0.625$ is depicted in Fig. 1. Note that while the droplet surface is not very smooth, there is no evaporation. For chains with $N_c = 4$, a lower temperature ($T^* = 0.57$) is required to keep droplets nonvolatile during spreading. An examina-

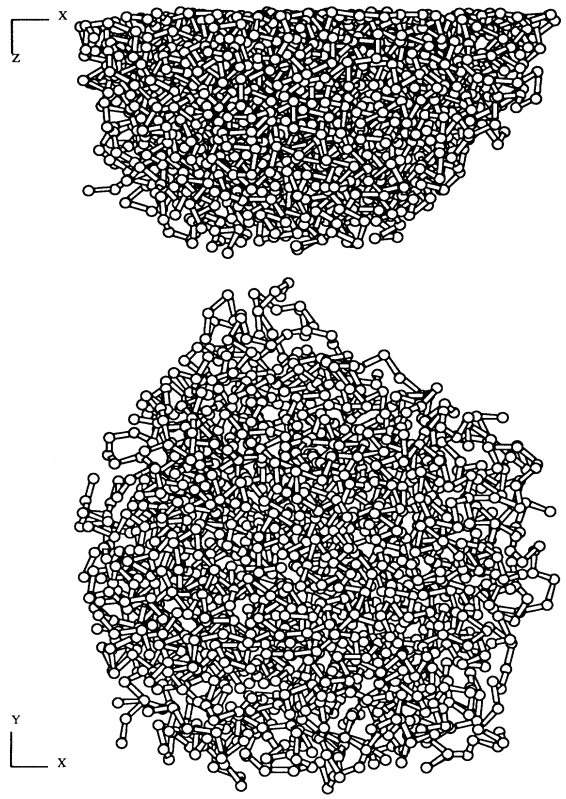

FIG. 1. A droplet with $N_c = 16$ in equilibrium at temperature $T^* = 0.75$ on a substrate of $\epsilon_w^* = 0.625$ viewed normally to the substrate and parallel to it.

tion of the diffusion of individual particles suggests that the core of the droplet is still liquid even at this lower temperature.

Figure 2 demonstrates that droplets are atomically layered, much as films [11] and droplets [12] of a simple LJ liquid and confined films of chain molecules [13] are layered. This figure presents a profile of the average density as a function of height. The inset shows the radial extent of the layers, and the region of low density near the edge of the droplet. The spacing in the z direction between density peaks is equal to the distance between atoms in a chain, suggesting that near the substrate, bonds between atoms in a chain tend to align at angles either near 0 or near $\pi/2$ to the surface normal.

TABLE I. Characterization of chains in the droplet by their moments. During an equilibrium simulation with parameters as for Figs. 1 and 2, time series were extracted of the radii of gyration of individual chains parallel and perpendicular to the substrate ($\Delta^2 r = [(x - x_{\text{c.m.}})^2 + (y - y_{\text{c.m.}})^2]/2$ and $\Delta^2 z = (z - z_{\text{c.m.}})^2$, respectively) and also the skewness perpendicular to the substrate [$S = (z - z_{\text{c.m.}})^3$] for 16 chains with their centers of mass in the lowest two atomic layers, for 16 chains with their centers of mass in a region above the third layer, and for 8 chains near the top of the droplet. The mean and standard deviation (from time and ensemble averages) of each of these quantities are tabulated below.

Location	$\Delta^2 r$	σ_r	$\Delta^2 z$	σ_z	S	σ_S
bottom	1.675	1.218	0.650	0.442	0.199	0.456
center	1.134	0.903	1.690	1.073	0.205	1.106
top	1.323	0.937	0.821	0.407	-0.185	0.523

The configurations of individual chains in a droplet in equilibrium are further characterized by the quantities in Table I. Broadly speaking, chains near the top and bottom of the droplet are flattened in the sense that a configuration which is extended in the z direction is much less likely than a configuration which is extended parallel to the substrate. Note that this flattening is not due to any shearing effect imposed by a mean flow.

The overall shape of an equilibrium droplet is controlled by the spreading parameter $S = \gamma_{SV} - \gamma_{LS} - \gamma_{LV}$, where the γ's are surface tensions between liquid, vapor, and solid. S is controlled by adjusting ϵ_w^*. For a

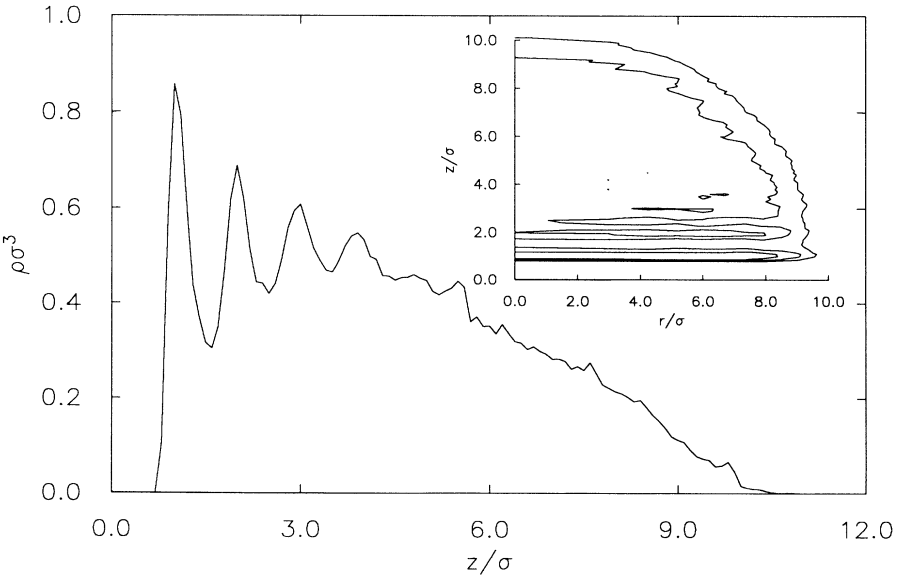

FIG. 2. Dimensionless density plotted versus distance perpendicular to substrate for a droplet with the same parameters as that shown in Fig. 1. Three distinct layers are discernible. The inset is a contour plot of the density in the same droplet, with contours $\rho\sigma^3 = 1/3, 2/3$, and 1.

more strongly attractive interface, the droplets are flattened, as may be seen in Fig. 3. While it is easy to extract a contact angle from the profiles in Fig. 3, it is not obvious that a contact angle so defined (that is, the contact angle for three or four atomic layers) is the same as the analogous macroscopic quantity. For ϵ_w^* large enough (i.e., large solid-liquid interfacial attraction), the fluid wets the substrate. At the temperatures and wall strengths used in our simulations, the wetting film is not an atomic monolayer— though molecules are constrained by the substrate, they still flop around through three-dimensional configurations.

We now turn to the dynamics of spreading droplets. To make a droplet spread, we take a droplet equilibrated for $\epsilon_w^* = 0.625$ (Figs. 1 and 2 show such droplets) and simply increase ϵ_w^* to 1.25. The liquid does not wet the substrate at $\epsilon_w^* = 1.04$, while it does wet the substrate at $\epsilon_w^* = 1.25$. Figure 4 shows a droplet of chains of length 16 in the process of wetting the substrate. While there are regions at the edge of the droplet where it is but a single atom thick, there is no well-defined precursor layer, even though chains at the edge of the droplet throughout the spreading period are flattened.

Figure 5 shows a tetramer droplet in an earlier phase of spreading than Fig. 4. Here, there is a layer entirely surrounding the droplet with a coverage only one atom thick. However, this layer is undergoing essentially two-dimensional evaporation as can be seen from Fig. 5. The chains which evaporate at the contact line are confined to the substrate, but not so strongly that they are restricted to two-dimensional configurations.

These results appear to be at least partially in agreement with the study of Nieminen and Ala-Nissila [14]; they also observe flattened chains in their simulations, but the droplets they show have a clear distinction between precursor film and core. They appear, however, to be working in a different regime. For them, the substrate potential strength which produces flattened chains in a well-defined precursor layer during spreading is much larger than for us [$\epsilon_w^*(\sigma_w^*)^3$ is 125 or 7.8 instead of our 1.8]. We are unable, however, to reconcile their characterization of all their droplets as nonvolatile at reduced

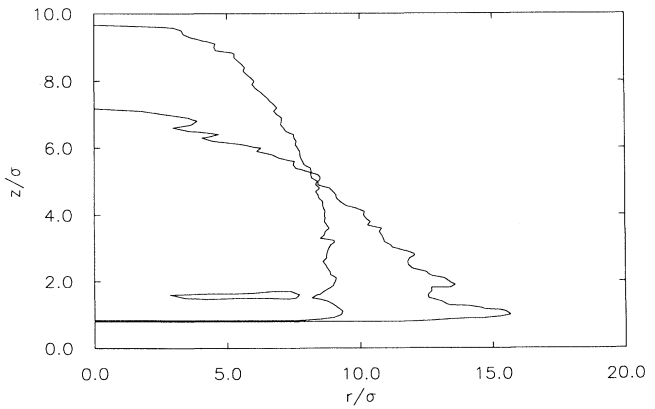

FIG. 3. Contours of $\rho\sigma^3 = 0.5$ for equilibrium droplets with $N_c = 16$ on substrates with $\epsilon_w^* = 0.625$ and 1.04.

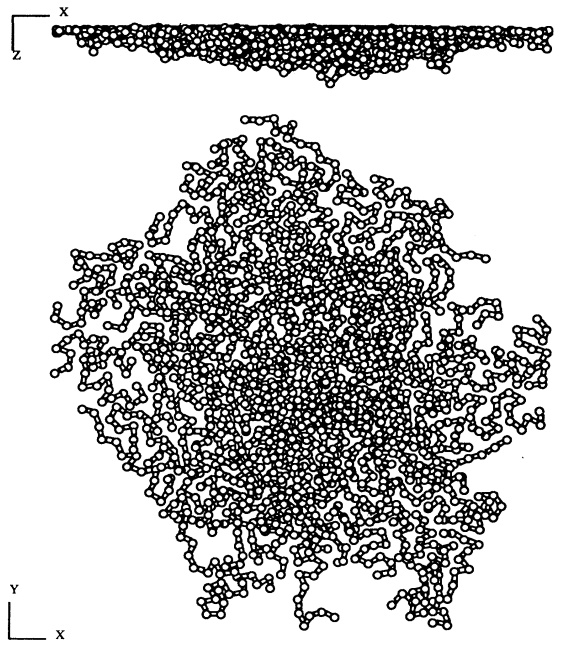

FIG. 4. A spreading droplet with $N_c = 16$ at temperature $T^* = 0.75$ on a substrate of $\epsilon_w^* = 1.25$ $t = 2482\tau$ after spreading began.

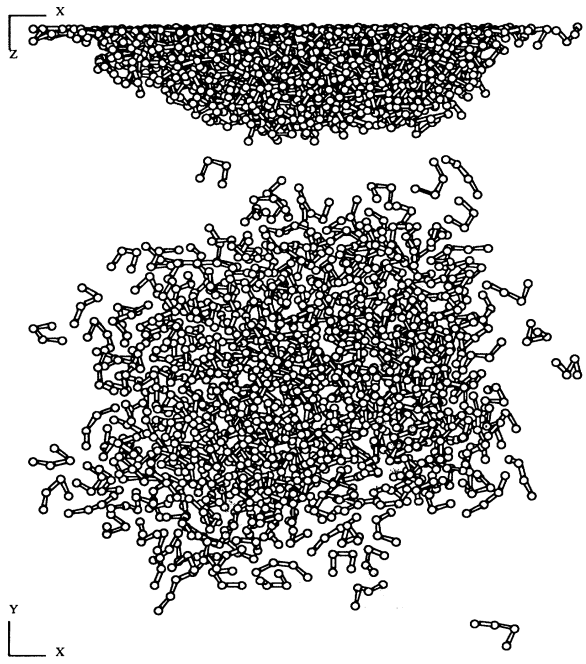

FIG. 5. A spreading droplet of tetramers at temperature $T^* = 0.57$ on a substrate of $\epsilon_w^* = 1.25$ $t = 707\tau$ after spreading began.

temperatures of 0.8 and 1.2 with either our simulations (we find some three-dimensional evaporation for tetramer droplets during spreading at $T^* = 0.68$), the simulations of Thompson *et al.* [10] on liquid drops in free space (who find a vapor phase for monomer droplets at $T^* = 0.76$), or the simulations of Yang *et al.* [12], who find evaporation for spreading monomer droplets at $T^* = 0.7$. Regardless of the strength of the substrate, it seems likely that some chains with $N_c \leq 4$ should break free, and certain that some monomers should do so, during a reasonable equilibration period before the droplet is brought into contact with the substrate.

A characterization of the motion of individual chains, both in static and spreading droplets, is uniquely accessible to molecular dynamics simulations. Figures 6(a) and 6(b) depict the motion of centers of mass of individual chains during the initial phase of the spreading. Each set of points represents an average of several runs, started from distinct initial conditions (an equilibrated droplet at $\epsilon_w^* = 0.625$ sampled at widely separated times) and allowed to evolve for 700τ. In order to identify whether the way chains move during the spreading process is qualitatively dependent on chain length (i.e., whether the degree of entanglement between chains changes the dynamics of spreading), we ran such simulations for droplets made of chains with $N_c = 16$ and $N_c = 4$. Figure 6(a) shows that the chains drift downwards uniformly throughout the lower part of a spreading droplet. Closer to the edge of the droplet (increasing $r - r_{CM}$), one finds a larger proportion of the chains close to the substrate (for such chains dz/dt is 0 on average), and a smaller absolute number of chains. Thus, on average, near the edge of the droplet dz/dt is noisy and close to 0.

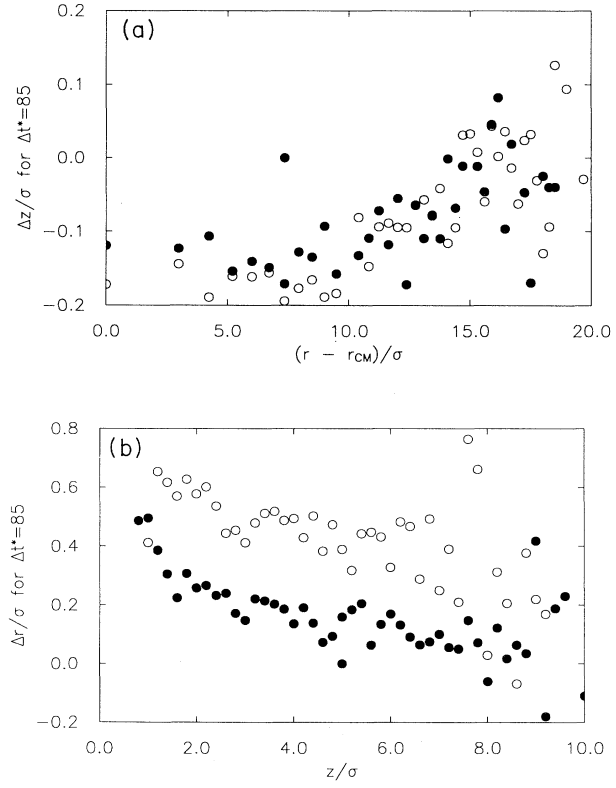

FIG. 6. Displacement of individual chains during spreading for $N_c = 4$ (full circles; average of six runs; $T^* = 0.57$; $\epsilon_w^* = 1.25$) and with $N_c = 16$ (open circles; average of eight runs $T^* = 0.57$; $\epsilon_w^* = 1.25$). (a) Displacement perpendicular to the substrate over an interval $\delta t = 85\tau$, averaged over the $t < 700\tau$ part of the spreading. Note that since even for tetramers the configuration at the end of the averaging period is not too flattened, the statistics are not too badly contaminated by chains that have reached substrate. Displacements are averaged only for $z < 4$, that is, in the lower three layers. (b) Displacement parallel to the substrate, averaged as in (a).

Figure 6(b) shows that chains at the bottom of the droplet spread more quickly than those at the top, with the smaller number of chains undergoing a weaker mean motion at the top of the droplet explaining the small mean and large variance of the motion there. The apparently surprising result that the mean radial motion of short chains, which one might expect to be more mobile, is slower than that of long chains is due to there being a larger fraction of short chains in the center of the droplet undergoing little or no radial motion.

This characterization of the motion of individual chains is not in agreement with the recent model of de Gennes and Cazabat [6] for the dynamics of spreading droplets. They model droplets of simple liquids as discrete layers of incompressible fluid with transport between layers occurring only near the edges of each layer. The width ξ of the region in which interlayer transport is expected scales as the square root of the reciprocal of the diffusion coefficient times viscosity. It is not *a priori* apparent how ξ will change in going from a simple liquid to a polymer liquid. If simple liquid droplets spread in a markedly different way from polymer droplets, however, one would expect to see some crossover behavior as chain length shortened. We see no such behavior. Also, even in the volatile simple liquid simulations of Yang *et al.* [12], atoms drift downward in the center of a large droplet. The other possibility for reconciling the predictions of [9] with our results is that $\xi \sim R$, the droplet radius. Interpreting ξ as a healing length, this seems unlikely, since for tetramer chains the healing length would need to be much larger than the chains themselves.

To conclude, we have studied the static and dynamic behavior of droplets composed of chain molecules with $N_c = 16$ and 4 at temperatures where the droplets are liquid but nonvolatile. We find the familiar phenomenon of layering in our droplets, and we find that chains near the top and bottom of the droplet are anisotropic. We find that the motion of individual chains in our (small) spreading droplets disagrees qualitatively with the prediction of a model for simple liquids based on interactions between incompressible fluid layers.

I have benefited from numerous discussions with Charles Ebner, ONR Grant No. N00014-92-J-1271, NSF Grants No. DMR-90154679 and No. DMR-9406936, and the use of the University of Minnesota Supercomputer Center's XMol computer program to generate several figures.

[1] F. Heslot, A.-M. Cazabat, P. Levinson, and N. Fraysse, Phys. Rev. Lett. **65**, 599 (1990).
[2] P. Silberzan and L. Léger, Phys. Rev. Lett. **66**, 186 (1991).
[3] U. Albrecht, A. Otto, and P. Lederer, Phys. Rev. Lett. **68**, 3192 (1992).
[4] M. P. Valignat, N. Fraysse, A.-M. Cazabat, and F. Heslot, Langmuir **9**, 601 (1993).
[5] P.-G. de Gennes, Rev. Mod. Phys. **57**, 827 (1985).
[6] P.-G. de Gennes and A.-M. Cazabat, C. R. Acad. Sci. Ser. II **310**, 1601 (1990).
[7] M. Sun and C. Ebner, Phys. Rev. A **46**, 4813 (1992).
[8] M. P. Allen and D. J. Tildesley, *Computer Simulation of Liquids* (Clarendon, Oxford, 1987).
[9] J.-P. Ryckaert, G. Cicotti, and H. J. C. Berendsen, J. Comput. Phys. **23**, 327 (1977).
[10] S. M. Thompson, K. E. Gubbins, J. P. R. B. Walton, R. A. R. Chantry, and J. S. Rowlinson, J. Chem. Phys. **81**, 530 (1984).
[11] J. P. Hansen and I. MacDonald, *Theory of Simple Liquids* (Academic, London, 1986).
[12] J. Yang, J. Koplik, and J. R. Banavar, Phys. Rev. Lett. **67**, 3539 (1991).
[13] P. A. Thompson, G. S. Grest, and M. O. Robbins, Phys. Rev. Lett. **68**, 3448 (1992).
[14] J. A. Nieminen and T. Ala-Nissila, Phys. Rev. E **49**, 4229 (1994).